JBC Papers in Press. Published on November 20, 2000 as Manuscript M006535200

ACTIVATION OF THE ENDOTHELIAL NITRIC OXIDE SYNTHASE BY TUMOUR NECROSIS FACTOR-α: A NOVEL FEED-BACK MECHANISM REGULATING CELL DEATH

Stefania Bulotta[*], Rico Barsacchi[°§], Domenicantonio Rotiroti[*], Nica Borgese[*§], and Emilio Clementi[°§#]

[*]Faculty of Pharmacy, University of Catanzaro "Magna Graecia", 88021 Roccelletta di Borgia, Italy; [°]Dept. Neuroscience-DIBIT H San Raffaele Institute, 20132 Milano, Italy; [§] CNR Centre of Cellular and Molecular Pharmacology, 20129 Milano, Italy; [#]Dept. Pharmaco-Biology, University of Calabria, 87036 Rende, Italy

Running Title: Tumour necrosis factor-α and endothelial nitric oxide synthase

Author for correspondence:

Dr. Emilio Clementi
DIBIT-H San Raffaele Institute
via Olgettina 58
20129 Milano
Italy
Tel: [*]39 02 2643 4807
Fax: [*]39 02 2643 4813

Abstract

Cell death via apoptosis induced by tumour necrosis factor-α (TNF-α) plays an important role in many physiological and pathological conditions. The signal transduction pathway activated by this cytokine is known to be regulated by several intracellular messengers. In particular, in many systems nitric oxide (NO) has been shown to protect cells from TNF-α-induced apoptosis. However, whether NO can be generated by the cytokine to down-regulate its own apoptotic programme has never been studied. We have addressed this question in HeLa Tet-off cell clones stably transfected with the endothelial NO synthase under a tetracycline-responsive promoter. Endothelial NO synthase, induced about 100-fold in these cells by removal of the antibiotic, retained the characteristics of the native enzyme of endothelial cells, both in terms of intracellular localisation and functional activity. Expression of the endothelial NO synthase was sufficient to protect from TNF-α-induced apoptosis. This protection was mediated by the generation of NO. TNF-α itself stimulated endothelial NO synthase activity to generate NO through a pathway involving its lipid messenger, ceramide. Our results identify a novel mechanism of regulation of a signal transduction pathway activated by death receptors and suggest that NO may constitute a built-in mechanism by which TNF-α controls its own apoptotic programme.

Introduction

Tumour necrosis factor α (TNF-α)[1], is a pleiotropic cytokine involved in the regulation of important physiological functions, including the development of tissues and the co-ordinate activation of immune responses, as well as in the onset and progress of pathological conditions (1-4). Most of these actions are exerted by TNF-α via its ability to induce cell death via apoptosis. This process is activated by the cytokine through the stimulation of its p55 kDa, type I receptor (TNF-RI), whose signal transduction pathway has been characterised in quite some detail. Binding of TNF-α results in receptor trimerisation with clustering of the cytosolic death domains, interaction with the complementary domains present in specific cytosolic proteins, including TRADD and FADD, and formation of the transduction complex, referred to as the DISC (5). This leads to the recruitment and proteolytic activation of a specific pro-protease, procaspase-8 (and possibly also -10) (5), which initiates a cascade of signalling events, including generation of the lipid metabolite ceramide, cytochrome c release from mitochondria, apoptosome formation as well as activation of downstream caspases, all of them integrated in an operational network leading to cell death (6-8).

The gaseous messenger nitric oxide (NO) plays a role in the modulation of TNF-α signalling. When generated after cytokine-stimulated expression of the inducible isoform of its synthesising enzymes, NO synthase (NOS), NO may contribute to later stages of apoptosis (see *e.g.* refs. 9-12; but see also 13). By contrast, administration of NO prior to, or together with TNF-α has been shown to inhibit apoptosis stimulated by the cytokine (13-

[1] List of abbreviations: $[Ca^{2+}]_i$, intracellular concentration of calcium; CHX, cycloheximide; DMEM, Dulbecco's modified Eagle medium; cGMP, guanosine 3':5'-cyclic monophosphate; Fum, fumonisin B1; MTT, 3-[4,5-dimethylthiazol-2yl]-2,5,-diphenylterazolium bromide; NO, nitric oxide; NOS and eNOS, nitric oxide synthase and its endothelial isoform; L-NAME, N^{ω}-nitro-L-arginine methyl ester; L-NMMA, N^{ω}-monomethyl-L-arginine; PDMP, DL-threo-1-phenyl-2decanoylamino-3morpholino-1-propanol; TNF-α and TNF-RI, tumour necrosis factor-α and its p55 receptor.

19). Two lines of evidence suggest that this early protective effect of NO might be of physiological relevance. First, NO acts by inhibiting key apoptogenic signal transduction events triggered by TNF-α, including ceramide accumulation and TRADD recruitment to the DISC complex, cytochrome c release, as well as the activity of initiator and effector caspases, both before and after their enzymatic cleavage (13-15, 17-19). Second, inhibition of endogenous NOS activity during stimulation with TNF-α increases apoptosis induction by the cytokine (18,20,21). A direct link between NOS activity and protection from TNF-α-induced apoptosis was demonstrated by infection experiments with the inducible isoform of NOS, an enzyme which generates NO continuously (16). These experiments, however, left open the question of whether endothelial and neuronal NOS, whose activity is instead regulated by intracellular messengers (22), would be stimulated to counteract the apoptogenic effect of TNF-α, and whether this would be sufficient to protect cells from death.

To address this question we have investigated cell death in response to TNF-α of a HeLa Tet-off cell line expressing bovine endothelial NOS (eNOS) in an inducible fashion. By comparing the degree of TNF-α-induced apoptosis in cells expressing or not expressing the enzyme, we were able to show that expression of eNOS is sufficient to induce a partially resistant phenotype, and that this effect is due to generation of NO. We have also investigated the mechanism of this resistance, and found that eNOS activity is stimulated by TNF-α itself through a pathway involving ceramide accumulation. Our study shows that eNOS activity is regulated by, and itself regulates, the apoptotic process triggered by TNF-α in a complex regulatory circuit.

Experimental procedures

Cell culture, transfection and selection of stable clones

Bovine eNOS cDNA, subcloned in pBluescript SK, was a kind gift of dr. William C. Sessa (Yale University School of Medicine, New Haven, CT). The cDNA was excised with EcoR1 and ligated in the EcoR1 site of plasmid pTRE (Clontech, Palo Alto, California). The orientation of the insert was checked by restriction mapping.

HeLa Tet-off cells (Clontech) were grown in Dulbecco's modified Eagle medium (DMEM) (Gibco BRL Life Technologies, Paisley, UK), supplemented with 10 % Tet System Approved FBS (Clontech), 50 UI/ml penicillin, 50 μg/ml streptomycin, 2 mM L-glutamine, 100 μg/ml G418 (Roche Diagnostics, Mannheim, Germany) and maintained at 37 °C under a 5 % CO_2 atmosphere.

Cells grown on 35 mm Petri dishes to ~ 40% confluence were co-transfected by the calcium phosphate method (23) using 0.5 μg of pTRE/eNOS plasmid and 25 ng of pTK-Hygr plasmid (Clontech) per cm^2 of culture dish. 3 days after transfection, the cells were detached with trypsin and plated in the presence of doxycycline hydrochloride (0.01-1 μg/ml) (Sigma, St. Louis, MO) and hygromycin B (200 μg/ml) (Roche Diagnostics). After 3 weeks, hygromycin-resistant colonies were expanded in 24-well Petri dishes.

Stable transfectants were maintained in medium supplemented with 100 μg/ml G418, 100 μg/ml hygromycin and 10 ng/ml doxycycline. To induce expression of eNOS, cells were plated in the absence of doxycycline. Unless otherwise specified, experiments were carried out on cells cultured for 72 h with or without the antibiotic.

A mouse endothelial cell line immortalised with the middle T antigen (E2 cells), a kind gift of Elisabetta Dejana (Mario Negri Institute, Milan, Italy) was maintained in culture as described (24)

Protein extraction and immunoblot analysis

Cell monolayers were washed free of medium, solubilised by direct addition of a pre-heated (to 80°C) denaturing buffer, containing 50 mM Tris-Cl pH 6.8, 2% SDS and a protease inhibitor cocktail (Complete, Roche Diagnostics), and immediately boiled for 2 min. After addition of 0.05% bromophenol blue, 10% glycerol and 2% β-mercaptoethanol, samples were boiled again and loaded onto 10% SDS-polyacrylamide gels. After electrophoresis, polypeptides were electrophoretically transferred to nitro-cellulose filters (Schleicher & Schuell, Dassel, Germany). Monoclonal anti-eNOS (Transduction Laboratories, Lexington, KY) and monoclonal anti-β-actin (Sigma) antibodies were used to reveal the respective antigens. After incubation with secondary reagent (polyclonal anti-mouse horseradish peroxidase conjugate, Transduction Laboratories), blots were developed with the enhanced chemiluminescence procedure (ECL-Plus; Amersham Pharmacia, Little Chalfont, UK).

Immunofluorescence and diaphorase cytochemistry

Cells plated on glass coverslips, fixed with 4% paraformaldehyde (Sigma) in 120 mM sodium phosphate, pH 7.4, for 30 min at 37°C, were permeabilised with Triton X-100 and processed for immunofluorescence as described previously (25). Cells were doubly immunostained with monoclonal anti-eNOS and anti-giantin polyclonal antibodies, the latter a kind gift of Dr. M. Renz (Institute of Immunology and Molecular Genetics, Karlsuhe, Germany; see ref. 26). Bound monoclonal and polyclonal antibodies were revealed by fluorescein-labelled anti-mouse IgG and rhodamine-conjugated anti-rabbit IgG (Jackson Immunoresearch Laboratories Inc., West Grove, PA). Preparations were observed under a Nikon Optiphot 2 microscope equipped for epifluorescence or with a Bio-Rad MRC 1024 laser confocal microscope.

For the diaphorase reaction cells, fixed as above, were incubated for 30 min at 37 °C in a buffer containing 100 mM Tris-Cl pH 7.4, 0.2% Triton X-100, 1 mM β-NADPH (Sigma)

and 0.2 mM nitro blue tetrazolium (Sigma), and observed by bright-field light microscopy (27).

Assay of NOS activity

NOS activity was assayed in both homogenised and intact cells by measuring the conversion of L-[^{3}H] arginine (Amersham Pharmacia) into L-[^{3}H] citrulline. In the first approach, HeLa or E2 cells were detached by trypsinisation, pelleted and resuspended (2 x 10^7 cells/ml) in an homogenisation buffer containing: 320 mM sucrose, 1 mM dithiothreitol, 1 mM EDTA, 20 mM HEPES, pH 7.2, supplemented with a protease inhibitor cocktail (Complete, Roche Diagnostic). After sonication (30 sec at 4°C), 50 µl of cell extract were assayed in a total volume of 150 µl as described (28). In some samples 500 µM N^{ω}-monomethyl-L-arginine (L-NMMA) or 1 mM EGTA were included. NOS activity in intact cells was measured on monolayers washed and then incubated for 20 min at 37°C in a reaction buffer containing: 145 mM NaCl, 5 mM KCl, 1 mM $MgSO_4$, 10 mM glucose, 1 mM $CaCl_2$ and 10 mM HEPES, pH 7.4, with or without N^{ω}-nitro-L-arginine methyl ester (L-NAME; 500 µM) (Sigma). In the experiments with fumonisin B1 (Fum) (10 µM; Sigma) or DL-threo-1-phenyl-2decanoylamino-3morpholino-1-propanol (PDMP) (50 µM; Calbiochem, Bad Soden, Germany) cell were pre-incubated for 3 h in culture medium containing the compounds, which were also added during the subsequent incubation in the reaction buffer. At the end of the pre-incubation, 2.5 µCi/ml of L-[^{3}H] arginine was added 5 minutes before cell stimulation with ATP (100 µM) or TNF-α (100 ng/ml; Alexis Italia, Florence, Italy). Non stimulated cells were run in parallel. 15 minutes later the monolayers were washed with 2 ml of ice-cold phosphate buffered saline, pH 7.4, supplemented with L-arginine (5 mM) and EDTA (4 mM). 0.5 ml of 100% cold ethanol was added to the dishes and left to evaporate before a final addition of 2 ml of 20 mM HEPES, pH 6.0. Separation of L-[^{3}H] citrulline from L-[^{3}H] arginine was obtained by DOWEX 50X8-400 chromatography (Sigma) as described (29). In the assay carried out with homogenised cells,

values obtained from samples incubated without cell extracts were subtracted. Data in the intact cells are presented without background correction. L-[^{3}H] citrulline formed was normalised to protein content (bicinchoninic acid assay, Pierce, IL).

Measurement of cGMP formation

NO-dependent guanosine 3':5'-cyclic monophosphate (cGMP) generation by the transfected HeLa clone Aδ was measured in both the cells themselves and in a co-incubation system using PC12 cells as a reporter system. PC12 cells were grown at 37°C, 5% CO_2 in DMEM supplemented with 10% heat-inactivated horse serum and 5 % Foetal Clone III, then detached by trypsinisation for the experiment. Samples of suspended 2 x 10^6 HeLa and 0.5 x 10^6 PC12 cells, either separate or together, were treated for 15 minutes at 37°C in the presence or absence of either ATP (100 μM), TNF-α (100 ng/ml) or S-nitroso acetyl penicillamine (100 μM; Calbiochem) in 1 ml of a solution containing: 125 mM NaCl, 5 mM KCl, 1.2 mM $MgSO_4$, 1.2 mM KH_2PO_4, 2 mM $CaCl_2$, 6 mM glucose, 1 mM L-arginine, 0.6 mM isobuthylmethylxanthine and 25 mM HEPES, pH 7.4, with or without L-NAME (500 μM). In the experiments with Fum (10 μM) and PDMP (50 μM), pre-incubations were for 3 h as described above. The reaction was terminated by addition of ice-cold trichloroacetic acid (final concentration 6%). After ether extraction, cGMP levels were measured using a radioimmunoassay kit (NEN™, Boston, MA) and normalised to cellular proteins as described above.

Induction and detection of cell death

HeLa cells seeded in 6-well plates (10^5 cells/cm^2) were incubated in the presence or absence of TNF-α (100 ng/ml) and cycloheximide (CHX; 1 μg/ml). In some samples L-NAME (500 μM) was also present. Cell death was measured using the colorimetric assay with 3-[4,5-dimethylthiazol-2-yl]-2,5-diphenyltetrazolium bromide (MTT; Sigma) (30). At

the end of the treatments, cell plates were washed with RPMI 1640 (without phenol red) and incubated for 3 h at 37 °C with 2.4 mM MTT in the same medium, the untransformed MTT carefully removed and the dye crystals solubilised in 1 ml of 2-propanol. Absorbance was read immediately in a UVIKON 941 spectrophotometer (test wave-length of 570 nm; reference wave-length of 690 nm).

Apoptosis was measured by flow cytometry using two different protocols as described (31). In the first approach, phosphatidyl serine exposure was monitored by staining for 15 min at room temperature with fluorescein-iso-thiocyanate-labelled annexin V (0.5 μg/ml in phosphate buffered saline). In the second approach the hypodiploid DNA peak in single parameter DNA histograms typical of apoptotic cells was identified. To this end, DNA was stained in unfixed cells incubated for 60 min at 37°C in 0.1% sodium citrate, 50 mg/ml propidium iodide, 100 μg/ml RNAse A (Sigma) and 0.01% Nonidet P40. Cells were analysed for either DNA content or annexin V staining using a fluorescence-activated cell sorter (FACStar Plus, Becton Dickinson, Sunnyvale, CA).

Measurement of ceramide concentration

Samples containing 2 x 10^6 HeLa cells were incubated at 37°C with or without PDMP (50 μM) and Fum (10 μM) for 3 h, then treated with TNF (100 ng/ml) for further 15 min. Conversion of ceramide to the ^{32}P-labelled ceramide phosphate was carried out by diacylglycerol kinase treatment of the extracted lipids in the presence of 10 μCi γ^{32}P-ATP as previously described (19). The ceramide phosphates produced were separated on a one-dimensional thin layer chromatography using chloroform/methanol/acetic acid (65:15:5; v/v/v) as solvent. The relevant spots were identified by autoradiography and their radioactivity measured by liquid scintillation counting. The concentration of ceramide per sample was determined vs. a standard curve encompassing the range of ceramide expected in the samples.

Statistical analysis

The results are expressed as means ± standard error of the mean (S.E.M.); *n* represents the number of individual experiments. Statistical analysis was carried out using the Student's *t* test for unpaired variables (two-tailed). The marks *, ** and *** or +, ++, +++ in the figure panels and tables refer to statistical probabilities (*P*) of < 0.05, < 0.01 and < 0.001, respectively, as detailed in the legends to figures and tables.

Results

Characterisation of HeLa Tet-off clones inducibly expressing eNOS

For our experiments we chose the Tet-off System (32), that allows repression of a single gene by tetracycline or a tetracycline derivative, such as doxycycline. After transfection of HeLa Tet-off cells with eNOS cDNA together with a plasmid conferring resistance to hygromycin, we expanded 30 resistant clones of which 6 expressed eNOS when doxycycline was removed from the medium as established by Western blotting and by immunofluorescence. Since the Tet-off System, by allowing comparison between the "on" and "off" states of the transfected cDNA, permits direct assessment of the consequences of the expression of a single gene in an internally controlled system, we carried out a detailed analysis on only one of the selected clones, clone Aδ.

We first analysed the time-course of eNOS induction by removal of doxycycline from the medium (Fig. 1 A). As shown in Fig. 1 A, the removal of doxycycline led to a rapid induction of the expression of eNOS, detectable as a 140 000 Mr band (arrow-head in Fig. 1 A), which was visible already at 4 h and continued to increase in intensity during the following 3 days. At the later time points, lower M_r bands appeared (see 24, 48 and 72 h time-points of Fig. 1 A); these were presumably products of eNOS proteolysis, since they were not present in non-induced cells (0 and 2 h time-points).

Next, we investigated the dependence of eNOS levels on doxycycline concentration. As can be seen from Fig. 1 B, induction was detectable at doxycyline concentrations ≤ 0.1 ng/ml (lanes 3-7). With decreasing doxycyline concentrations, the expression of the enzyme gradually increased, to reach a maximum at an antibiotic concentration of 0.001 ng/ml.

To obtain a semiquantitative evaluation of the degree of induction of eNOS expression by doxycyline removal, we compared by Western blotting 30 μg of total protein extract from cells grown in the presence of doxycycline with different quantities of extract from cells grown in the absence of the antibiotic (Fig. 1 C). By loading a large amount of protein and by increasing exposure time of the blot, it was possible to detect a faint eNOS band in non induced cells, due to basal expression of the cloned cDNA (lane 1). This band was much less prominent than that obtained with 1/10 the amount of lysate from induced cells, whereas it was of intensity comparable to that of the band from 1/100 this amount of lysate (0.3 μg protein, lane 3). This result indicates that in response to doxycycline removal from the medium, this clone exhibits an approximately 100-fold induction of eNOS expression.

We also compared the level of eNOS expression in induced cells with that of endogenous eNOS in a murine endothelial cell line (E2 cells). As shown in Fig. 1 D, the level of eNOS in induced clone Aδ cells (lane 1) was only slightly higher compared to the endothelial cell line (lanes 2 and 3).

To investigate whether eNOS localisation in induced cells corresponds to that of the endogenous enzyme in endothelial cells (33), we carried out immunofluorescence analysis. As shown in Fig. 2 A, eNOS appeared most concentrated on the surface and in a perinuclear structure in the Golgi region of the cells, as shown by staining for the Golgi marker giantin in the same field of cells (Fig. 2 B). Confocal analysis (panels D, E and F) confirmed the Golgi localisation of eNOS, as is apparent by the yellow colour in the merged image of the double-stained cells (F).

We then analysed the Ca^{2+}-dependent activity of eNOS in homogenised and intact cells, by measuring the conversion of its substrate, L-arginine, into L-citrulline. As shown in Fig 3

A, citrulline formation in eNOS-expressing (dox-) cells was stimulated by Ca^{2+} (363 ± 4.1 %, n = 4 over the activity in the presence of EGTA). The Ca^{2+}-dependent activity was ~ 2.5 pmol/mg min^{-1} a value approximately threefold higher than those reported in the literature for endothelial cells (see e.g. 34). We also obtained similar activity values in the E2 cell extracts (not shown). The Ca^{2+}-dependent NOS activity was nearly completely abolished by the NOS inhibitor L-NMMA. In cells grown in the presence of doxycycline, instead, neither EGTA nor L-NMMA induced significant changes in citrulline formation.

In intact cells (Fig. 3 B), NOS activity was stimulated using ATP, an agonist of P_{2y} receptors known to increase $[Ca^{2+}]_i$ in HeLa cells. ATP increased L-citrulline formation with respect to untreated controls only in eNOS-expressing (dox-) cells, and this effect was prevented by the NOS inhibitor L-NAME, In contrast, no changes were observed in cells cultured in the presence of doxycycline (Fig. 3 B). The amplitude of the $[Ca^{2+}]_i$ increase induced by ATP (measured with fura-2, see ref. 35) was similar in dox- and dox+ cells (not shown).

We also carried out a morphological analysis of the diaphorase activity of eNOS. As shown in Fig. 3 C, the NADPH-dependent reduction of nitro blue tetrazolium generated a dark precipitate in eNOS-expressing cells grown in the absence of doxycyline (panel b), whereas cells cultured in the presence of the antibiotic remained colourless (panel a). The localisation of the precipitate in induced cells was reminiscent of that of the enzyme itself detected by immunofluorescence (Fig. 2).

To investigate whether eNOS-expressing cells are able to generate bioactive NO, we measured formation of cGMP, a good proxy for NO since soluble guanylate cyclase is activated by nanomolar concentrations of the gas (36). Exposure to ATP (15 min) of cells grown in the presence of doxycycline did not result in any increase in cGMP over non stimulated controls (0.36 ± 0.02 and 0.35 ± 0.03 pmol/mg min^{-1}, respectively; n = 4). In eNOS-expressing cells, administration of ATP resulted in a slight increase in cGMP formation over controls (0.44 ± 0.03 and 0.33 ± 0.01 pmol/mg min^{-1}, respectively; n = 3)

which was not observed in the presence of L-NAME (0.28 ± 0.02 pmol/mg min^{-1}), suggesting that these cells express low levels of guanylate cyclase. Therefore, in order to detect generation of cGMP, we used another cell type, the pheochromocytoma PC12, as a reporter system. These cells were chosen because they respond to NO with generation of cGMP (0.33 ± 0.04 and 9.45 ± 0.1 pmol/mg min^{-1} in controls and cells incubated with 100 μM of the NO donor S-nitroso acetyl penicillamine, $n = 3$, $P < 0.001$), whereas they do not generate cGMP when treated with ATP (not shown). As shown in Fig. 3 D, co-incubation of eNOS-expressing (dox-) HeLa cells together with PC12 cells resulted in an increased generation of cGMP after administration of ATP, which was inhibited by the presence of L-NAME. No changes in cGMP formation were observed with cells grown in the presence of doxycycline (Fig. 3 D).

eNOS expression inhibits TNF-α-induced cell death

To investigate the effects of the expression of eNOS on TNF-α-induced cell death, cells grown in the presence or absence of doxycyline were treated with TNF-α together with the protein synthesis inhibitor CHX for 6 h. In cells grown in the presence of doxycyline this treatment resulted in death as measured by the decreased conversion of MTT into formazan (Table I). eNOS-expressing (dox-) cells were less sensitive to death induction by TNF-α/CHX. However, when these cells were exposed to TNF-α/CHX in the presence of L-NAME, cell sensitivity to the treatment was similar to that observed in cells not expressing eNOS (Table I). The effect of L-NAME on eNOS-expressing cells was due to its inhibition of eNOS activity since the compound was without any appreciable effect in dox+ cells (Table I).

To further characterise the protective effect of eNOS expression, we measured, by flow cytometry, an early feature of apoptosis, i.e. the appearance of phosphatidyl serine on the outer leaflet of the plasma membrane, as well as another apoptosis hallmark, the formation of hypodiploid DNA. Phosphatidyl serine, measured by annexin V staining, was not

detected in cells either in the presence or absence of doxycycline (Fig. 4 A, a and c, respectively, Table II). Incubation with TNF-α/CHX (12 h) resulted, in both cell preparations, in the appearance of phosphatidyl serine (Fig. 4 A, panels b and d, respectively), however to a significantly lower extent in eNOS-expressing cells (panel d, Table II). Similarly, the increase of hypodiploid DNA after treatment with TNF-α/CHX observed in cells grown in the presence of doxycycline was significantly higher than that in dox- cells (Fig. 4 B, panels g h, and i l, respectively; Table II). When eNOS-expressing cells were exposed to TNF-α/CHX in the presence of L-NAME, the appearance of both phosphatidyl serine (Fig. 4 A, f) and hypodiploid DNA (Fig. 4 B, m) was significantly enhanced and not significantly different from that observed in non-induced (dox+) cells. The effect of L-NAME was specific because incubation with this compound had no appreciable action in dox+ cells (Table II).

Stimulation with TNF-α increases eNOS activity and NO generation

In order to investigate whether generation of NO from eNOS was induced as a consequence of cell stimulation with TNF-α, we measured the effect of a 15 min stimulation with the cytokine (in the absence of CHX) on NOS activity in intact HeLa cells and the generation of cGMP in the PC12 cell reporter system. As shown in Fig 5 A, NOS activity was stimulated by TNF-α in eNOS-expressing (dox-) HeLa cells. Consistently, these cells, when stimulated by the cytokine, caused increased cGMP generation in co-incubated PC12 cells (Fig. 5 B). Both these effects were prevented by L-NAME. In addition, TNF-α did not have any effect on NOS activity and cGMP generation when HeLa cells grown in the presence of doxycycline were used.

We considered the mechanism by which TNF-α stimulates eNOS activity. TNF-α is not known to increase $[Ca^{2+}]_i$, the best known activator of eNOS (22). In accordance, we did not detect any increases in $[Ca^{2+}]_i$ in HeLa cells during a 15 min stimulation with the cytokine (not shown). Generation of ceramide is among the intracellular events involved in induction

of apoptosis by TNF-α (6). Since short-chain analogues of this lipid messenger have been reported recently to activate eNOS (37), we investigated whether ceramide could be involved in the activation of eNOS by TNF-α. To this end we preincubated the cells with the ceramide synthase inhibitor, Fum, and the glycosylceramide synthase inhibitor, PDMP, which are known to decrease and increase, respectively, the generation of ceramide by TNF-α, presumably by altering the levels of substrate for sphingomyelinases (19, 38, 39).

The data of Table III show that ceramide levels in Aδ cells were affected by TNF-α, Fum and PDMP in the same way as described for other cells (19, 38, 39). TNF-α caused an early increase in ceramide concentration, which was augmented by preincubation with PDMP and diminished by Fum. These compounds had no significant effect on basal levels of ceramide.

We then proceeded to investigate the effects of Fum and PDMP on TNF-α-induced activation of eNOS. In the absence of TNF-α, Fum and PDMP did not modify NOS activity and cGMP formation in either eNOS-expressing or not expressing cells (not shown). These compounds had no effect also when given in combination to TNF-α to HeLa cells not expressing eNOS (Fig. 5; dox+). However, similarly to the effects on ceramide generation, PDMP enhanced, and Fum reduced the stimulatory effect of TNF-α on NOS activity in the induced cells (Fig. 5; dox -), suggesting that eNOS activation by TNF-α is mediated through a pathway involving ceramide.

Discussion

The aim of this study was to investigate the interaction between eNOS and TNF-α, and the effect of this interaction on TNF-α-induced cell death via apoptosis. To do this we have chosen HeLa cells because they express TNF-RI and die via apoptosis when treated with TNF-α (40, 41). We generated clones stably transfected with the eNOS cDNA under the control of a doxycycline-responsive promoter, in which transcription of the mRNA and

expression of the protein, suppressed in the presence of the antibiotic, is initiated by its removal, at levels inversely proportional to the concentration of antibiotic. The induced eNOS localised mainly to the plasma membrane and to the Golgi complex, was positive for NADPH diaphorase staining and showed a Ca^{2+}-dependent activity in HeLa cell extracts, at levels comparable to those of the endogenous enzyme in endothelial cells. In addition, ATP, which increases $[Ca^{2+}]_i$, stimulated eNOS activity with generation of bioactive NO, the latter assessed by formation of cGMP in a PC12 cell reporter system. These observations indicate that eNOS, when induced in HeLa cells, retains the intracellular distribution and functional characteristics of the native enzyme (33,34,42). Thus, eNOS Tet-off HeLa clones represent a clean, well-controlled system to study the interaction between eNOS and TNF-α, and the effect of this interaction on apoptosis, because all differences observed between cells cultured with or without doxycycline can be attributed to the presence/absence of the enzyme.

The protective effect of NO on TNF-α-induced apoptosis, when the gas was administered together with or prior to the cytokine, had already been shown in several studies. This effect of NO, however, had been demonstrated using either NO donors or continuous fluxes of endogenous NO, generated as a consequence of constitutive expression of inducible NOS after adenoviral gene transfer (13-19). These studies, therefore, did not establish whether generation of NO could be a built-in, physiological mechanism triggered by TNF-α to modulate its own apoptotic effect. To elucidate this, we have studied cell death induced by the cytokine, in the presence of the protein synthesis inhibitor CHX, in cells either expressing or devoid of eNOS. In particular, we measured the activity of mitochondrial dehydrogenases and two markers of apoptosis, *i.e.* the cell surface appearance of phosphatidyl serine and the formation of hypodiploid DNA. Our results show that induction of eNOS is sufficient per se to reduce significantly, yet not to abolish, the degree of cell death induced by TNF-α. This partial protection was eliminated by the NOS inhibitor L-NAME, indicating that the action of eNOS was due to generation of NO.

This generation of NO was due to stimulation of eNOS by TNF-α, and was already observed in the first minutes after its administration. Taken together, these results demonstrate that, in cells endowed with eNOS, the apoptotic programme triggered by TNF-α is modulated through the autocrine generation of NO induced by the cytokine.

To elucidate the pathway responsible for the TNF-α-induced generation of NO we have taken into consideration intracellular events known to stimulate eNOS. TNF-α did not induce any changes in $[Ca^{2+}]_i$, thus excluding the cation as the intracellular mediator. We concentrated on ceramide as a possible messenger since it is generated by TNF-α (6) and its short-chain analogues can stimulate eNOS (37). To investigate the role of ceramide we used PDMP and Fum, inhibitors respectively of glycosylceramide synthase and ceramide synthase, which increased and decreased, respectively, the early wave of ceramide generation induced by TNF-α in our Tet-off Hela cells. PDMP increased, while Fum inhibited the stimulation by TNF-α of eNOS activity and cGMP generation, suggesting that ceramide is involved in the activation of eNOS by TNF-α. Other mechanisms, however, may also play a role. In particular, Akt kinase has been shown recently to phosphorylate, and thus activate eNOS (42,43), and in some, although not in all cell systems, TNF-α may stimulate this kinase (44,45). It should be mentioned, however, that ceramide inhibits Akt kinase (46,47) so that it is unlikely that this enzyme plays a major role in the activation of eNOS by TNF-α reported here.

Several lines of evidence suggest that generation of ceramide by TNF-α plays an important role in the induction of apoptosis by the cytokine. In particular, impairment of the activity of sphingomyelinases, which generate ceramide following TNF-α stimulation, reduces the ability of the cytokine to induce apoptosis (48-52). In addition, short-chain ceramide analogues increase cell sensitivity to TNF-α (19,53). Recently, we have demonstrated that this is due at least in part to stimulation, by ceramide, of the recruitment of TRADD to TNF-RI with subsequent increased activation of caspase-8, a process which

occurs shortly (a few minutes) after receptor activation (19). Of importance, exogenous NO was able to prevent these effects of ceramide by inhibiting the TNF-α-induced accumulation of the lipid messenger. Now we show that, in cells endowed with eNOS, TNF-α induces an early stimulation of the enzyme activity in a ceramide-dependent way. Taken together, these results suggest that ceramide and NO constitute a two-messenger system, triggered by TNF-α to regulate bidirectionally the initial steps of its own apoptotic signalling pathway. A model for this mechanism of regulation is described in Fig. 6.

In the present study the mechanisms by which endogenously generated NO protects cells from TNF-α-stimulated apoptosis have not been investigated. Although the model of Fig. 6 focuses on the NO-ceramide feedback loop, it is likely that more than one of the effects described for exogenous NO, such as inhibition of caspase activity, Bcl-2 cleavage and cytochrome c release (13-15, 17-19), in addition to inhibition of ceramide formation (19), are relevant also to the action of endogenous NO. Among the substrates of NO, particularly relevant is caspase-3 because of its role as a central effector in many apoptotic pathways (7). Recent evidence with CD95 indicates that the inhibition of caspase-3 cleavage by S-nitrosylation, and the removal of this inhibition by activation of the death receptor, act as a switch to turn the apoptotic programme on (54). Furthermore, NO-dependent inhibition of caspase-3 cleavage, observed in endothelial cells when eNOS activity was increased by shear stress, was found to protect from apoptosis induced by various stimuli (20). Thus, in situations in which other apoptogens are present together with TNF-α, such as during inflammation, the functional coupling of the cytokine with eNOS we have shown, might act as a broad regulator of apoptosis.

Acknowledgements

We thank Jacopo Meldolesi for his critical revision of the manuscript; Rosaria Arcone Clara Sciorati and Vittorio Colantuoni for their help during the initial stages of this work; William Sessa and Elisabetta Dejana for their gifts of eNOS cDNA and E2 cells,

respectively; Teresa Sprocati for her assistance with the preparation of the illustrations. This work was supported by grants from: Italian Association for Cancer Research (E.C.); Consiglio Nazionale delle Ricerche, Target Project Biotechnology (E.C.); Ministero dell'Università e della Ricerca Scientifica e Tecnologica, Cofinanziamento 99 (E.C.); Schering-Plough Italia (E.C.); Armenise-Harvard Foundation (E.C.); Programma Operativo Plurifondo 1994/99, Regione Calabria (D.R.).

References

1. Aggarwal, B. B. and Natarajan, K. (1996) *Eur. Cytokine Ntw.* **7**, 93-124

2. Pan W, Zadina, J. E., Harlan, R. E., Weber, J. T., Banks, W. A. and Kastin, A. J. (1997) *Neurosci. Biobehav. Rev.* **21**, 603-613

3. Bradham, C. A., Plümpe, J., Manns, M. P., Brenner, D. A. and Trautwein, C. (1998) *Am. J. Physiol.* **275**, G387-G392

4. Meldrum, D. R. (1998) *Am. J. Physiol*. **274**, R577-R595

5. Ashkenazi, A. and Dixit, V. M. (1998) *Science* **281**, 1305-1308

6. Hannun, Y. A. (1996) *Science* **274**, 1855-1859

7. Green, D.R. (1998) *Cell* **94**, 695-698

8. Borner, C., Monney, L., Olivier, R., Rossé, T., Häcki, J. and Conus, S. (1999) *Cell Death Differ*. **6**, 201-206

9. Maciejewski, J. P., Selleri, C., Sato, T., Cho, H. J., Keefer, L. K., Nathan, C. F. and Young, N. S. (1995) *J. Clin. Invest.* **96**, 1085-1092

10. Binder, C., Schülz, M., Hiddemann, W. and Oellerich, M. (1999) *Lab. Invest.* **79**, 1703-1712

11. Chung, K. C., Park, J. H., Kim, C. H. and Ahn, Y. S. (1999) *J. Neurochem*. **72**, 1482-1488

12. Song, W., Lu, X. and Feng, Q. (2000) *Cardiovasc. Res.* **45**, 595-602

13. Kim, Y.-M., Talanian, R. and Billiar, T. R. (1997) *J. Biol. Chem.* **272**, 31138-31148

14. Dimmeler, S., Haendeler, J., Nehls, M. and Zeiher, A. M. (1997*) J. Exp. Med*. **185**, 601-607

15. Kim, Y.-M., Kim, T. H., Seol, D. W., Talanian, R. V. and Billiar, T. R. (1998) *J. Biol. Chem.* **273**, 31437-31441

16. Tzeng, E., Billiar, T. R., Williams, D. L., Li, J., Lizonova, A., Kovesdi, I. and Kim, Y. M. (1998) *Surgery* **124**, 278-283

17. Fiorucci, S., Antonelli, E., Santucci, L., Morelli, O., Miglietti, M., Federici, B., Mannucci, R., Del Soldato, P. and Morelli, A. (1999) *Gastroenterol.* **116**, 1089-1106

18. Li, J., Bombeck, C. A., Yang, S., Kim, Y.-M. and Billiar, T. R. (1999) *J. Biol. Chem.* **274**, 17325-17333

19. De Nadai, C., Sestili, P., Cantoni, O., Lièvremont, J.-P., Sciorati, C., Barsacchi, R., Moncada, S., Meldolesi, J. and Clementi, E. (2000) *Proc. Natl. Acad. Sci. USA* **97**, 5480-5485

20. Dimmeler, S., Hermann, C., Galle, J. and Zeiher, A. M. (1999) *Arterioscler. Thromb. Vasc. Biol.* **19**, 656-664

21. Agnoletti, L., Curello, S., Bachetti, T., Malacarne, F., Gaia, G., Comini, L., Volterrani, M., Bonetti, P., Parinello, G., Cadei, M., Grigolato, P. G. and Ferrari, R. (1999) *Circulation* **100**, 1983-1991

22. Stuehr, D. J. (1999) *Biochim. Biophys. Acta* **1411**, 217-230

23. Graham, F. L. and van der Eb, A. J. (1973) *Virol.* **52**, 456-467

24. Balconi, G., Spagnuolo, R. and Dejana, E. (2000) *Arterioscler. Thromb. Vasc. Biol.* **20**, 1443-1451

25. De Silvestris, M., D'Arrigo, A. and Borgese, N. (1995) *FEBS Lett.* **370**, 69-74

26. Seeling, H. P., Scheanz, P., Schroter, H., Wiemann, C. and Renz, M. (1994) *J. Autoimmun*. **7**, 67-91

27. Dawson, T. M., Bredt, D. S., Fotuhi, M., Hwang, P. M. and Snyder, S. H. (1991) *Proc. Natl. Acad. Sci. USA* **88**, 7797-7801

28 Lièvremont, J.-P., Sciorati, C., Morandi, E., Paolucci, C., Bunone, G., Della Valle, G., Meldolesi, J. and Clementi, E. (1999) *J. Biol. Chem.* **274**, 15466-15472

29. Bredt, D. S. and Snyder, S. H. (1989) *Proc. Natl. Acad. Sci. USA* **86**, 9030-9033

30. Denizot, F. and Lang, R. (1986) *J. Immunol. Methods* **89**, 271-277

31. Sciorati, C., Rovere, P., Ferrarini, M., Heltai, S., Manfredi, A. A. and Clementi, E. (1997) *J. Biol. Chem.* **272**, 23211-23215

32. Gossen, M. and Bujard, H. (1992) *Proc. Natl. Acad. Sci. USA* **89**, 5547-5551

33. Sessa, W. C., Garcìa-Cardeña, G., Liu, J., Keh, A., Pollock, J. S., Bradley, J., Thiru, S., Braverman, I. M. and Desai, K. M. (1995) *J. Biol. Chem.* **270**, 17641-17644

34. Shaul, P. W., Smart, E. J., Robinson, L. J., German, Z., Yuhanna, I. S., Ying, Y., Anderson, R. G. and Michel, T. (1996*) J. Biol. Chem.* **271**, 6518-6522

35. Clementi, E, Vecchio, I., Corasaniti, M.T. and Nisticò, G. (1995) *Eur. J. Pharmacol.* **289**, 113-123

36. Denninger, J. W. and Marletta, M. A. (1999) *Biochim. Biophys. Acta* **1411**, 334-350

37. Igarashi, J., Thatte, H. S., Prabhakar, P., Golan, D. E. and Michel, T. (1999) *Proc. Natl. Acad. Sci. USA* **96**, 12583-12588

38. Rani, C. S., Abe, A., Chang, Y., Rosenzweig, N., Saltiel, A. R., Radin, N. S. and Shayman, J. A. (1995) *J. Biol. Chem.* **270**, 2859-2867.

39. Laouar, A., Glesne, D. and Huberman, E. (1999) *J. Biol. Chem.* **274**, 23526-23534.

40. Meikrantz, W., Gisselbrecht, S., Tam, S.W. and Schlegel, R. (1994) *Proc. Natl. Acad. Sci. USA* **91**, 3754-3758

41. Castellino, A. M., Parker, G. J., Boronekiv, I. V., Anderson, R. A. and Chao, M. V. (1997) *J. Biol. Chem.* **272**, 5861-5870

42. Fulton, D., Gratton, J.-P., McCabe, T. J., Fontana, J., Fujio, Y., Walsh, K., Franke, T. F., Papapetropoulos, A. and Sessa, W. C. (1999) *Nature* **399**, 597-601

43. Dimmeler, S., Fleming, I., Fisslthaler, B., Hermann, C., Busse, R. and Zeiher, A. M. (1999) *Nature* **399**, 601-605

44. Ozes, O. N., Mayo, L. D., Gustin, J. A., Pfeffer, S. R., Pfeffer, L. M. and Donner, D. B. (1999) *Nature* **401**, 82-85

45. Romashkova, J. A. and Makarov, S. S. (1999) *Nature* **401**, 86-89

46. Zhou, H., Summers, S. A., Birnbaum, M. J. and Pittman, R. N. (1998) J. *Biol. Chem*. **273**, 16568-16575

47. Schubert, K. M., Scheid, M. P. and Duronio, V. (2000) J. *Biol. Chem*. **275**, 13330-13335

48. Wright, S. C., Zheng, H. and Zhong, J. (1996). *FASEB J.* **10**, 325-332.

49. Cai, Z., Bettaieb, A., Mahdani, N. E., Legres, L. G., Stancou, R., Masliah, J. and Chouaib, S. (1997) *J. Biol. Chem.* **272**, 6918-6926.

50. Bezombes, C., Maestre, N., Laurent, G., Levade, T., Bettaieb, A. and Jaffrezou, J.-P. (1998) *FASEB J.* **12**, 101-109.

51. Liu, B., Andrieu-Abadie, N., Levade, T., Zhang, P., Obeid, L.M. and Hannun, Y.A. (1998) *J. Biol. Chem.* **273**, 11313-11320.

52. Schütze, S., Machleidt, T., Adam, D., Schwandner, R., Wiegmann, K., Kruse, M.-L., Heinrich, M., Wickel, M. and Krönke, M. (1999) *J. Biol. Chem.* **274**, 10203-10212.

53. Higuchi, M., Singh, S., Jaffrezou, J.-P. and Aggarwal, B. B. (1996) *J. Immunol.* **156**, 297-304.

54. Mannick, J. B., Hausladen, A., Liu, L., Hess, D. T., Zeng, M., Miao, Q., Kane, L. S., Gow, A. J. and Stamler, J. S. (1999) *Science* **284**, 651-654

55. Rodriguez, A. and Flemington, E. K. (1999) *Anal. Biochem.* **272**, 171-181

56. Brenner, B., Ferlinz, K., Grassme, H., Weller, M., Koppenhoefer, U., Dichgans, J., Sandhoff, K., Lang, F. and Gulbins, E. (1998) *Cell Death Differ.* **5**, 29-37.

57. Dbaibo, G. S., Perry, D. K., Gamard, C. J., Platt, R., Poirier, G. G., Obeid, L. M. and Hannun, Y. A. (1997) *J. Exp. Med.* **185**, 481-490

58. Hannun, Y. A. and Luberto, C. (2000) *Trends Cell Biol.* **10**, 73-80

59. Garcia-Cardeña, G, Oh, P., Schnitzer, J. E. and Sessa, W. C. (1996) *Proc. Natl. Acad. Sci. USA* **95**, 6448-6453

60. Ko, Y.-G., Lee, J.-S., Kang, Y.-S., Ahn, J.-H. and Seo, J.-S. (1999) *J. Immunol.* **162**, 7217-7223

Footnotes

S.B. and R.B. contributed equally to this work.

Figure Legends

Fig. 1. Immunoblots of proteins extracted from clone Aδ. A: time-course of eNOS induction by removal of doxycycline from the medium. Aδ cells were grown in 100 mm dishes to 80% confluence in the presence of doxycycline (10 ng/ml). At time 0 cells were washed with phosphate buffered saline, split into smaller culture dishes (1/20th of the initial cultures per 35-mm dish), and incubated further in the absence of the antibiotic. At the indicated time-points, cells were harvested and analysed by 9% SDS-PAGE followed by electroblotting. ~10 μg of total cellular protein were loaded onto each lane. Protein load was checked by β-actin immunostaining, shown in the lower part of the panel. B: Dependence of eNOS expression on doxycyline concentration. Cells grown in the presence of doxycycline were split as described for panel A and then cultured in the presence of 1, 0.5, 0.1, 0.05, 0.01, 0.001 and 0 ng/ml of doxycycline (lanes 1-7, respectively) for 72 h. Shown is a

Western blot, in which ~10 μg of total protein for each condition were analysed. The lower part of the panel shows β-actin immunostaining of the same samples. C: semiquantitative evaluation of induction of eNOS expression by doxycycline depletion. Lysates were prepared from cells grown in the presence or absence of the antibiotic for 72 h. Lane 1 contained 30 μg protein of total extract from cells grown in the presence of doxycycline, whereas lane 2 and 3 contained 3 μg and 0.3 μg, respectively. Removal of doxycycline results in a ~100-fold induction of eNOS expression. D: comparison of eNOS levels in induced Aδ and E2 cells. The indicated amounts of proteins from Aδ cells (lane 1) and E2 cells (lanes 2 and 3) were loaded. In all panels, the arrow-head indicates eNOS (M_r 140 000), whereas the asterisk in panels A, B and D indicate β-actin immuno-staining for the same samples. Numbers on the left represent $M_r \times 10^{-3}$ of molecular weight standards from BioRad Laboratories (Richmond, CA).

Fig. 2. Double-staining immunofluorescence of clone Aδ cells. Cells expressing eNOS were doubly stained with monoclonal anti-eNOS and polyclonal anti-giantin antibodies followed by fluorescein-labelled anti-mouse IgG (A and D) and rhodamine-conjugated anti-rabbit IgG (B and E), respectively. Panels A, B, C show the same field of cells viewed under the fluorescein filter for eNOS (A), the rhodamine filter for giantin (B) and in phase contrast (C). eNOS (A) appears concentrated on the surface and in a perinuclear structure corresponding to the Golgi region, as shown by the giantin staining (B). Panels D, E, F show the same field of cells analysed by confocal microscopy: fluorescein (eNOS -D), and rhodamine (giantin -E) fluorescence are superimposed on the transmitted light image; co-localisation of the two is demonstrated by the yellow colour in the merged image (F). Bar, panels A, B, C, 15 μm; panels D, E, F, 10 μm.

Fig. 3. Characterisation of eNOS activity in clone Aδ. A: calcium dependency of eNOS activity in cell lysates. Lysates, prepared from cells grown in the presence (dox+) or absence

(dox-) of doxycycline for 72 h, were resuspended in a buffer containing L-[^{3}H] arginine and either 0.45 mM $CaCl_2$ (Ca^{2+}), 0.45 mM $CaCl_2$ and 1 mM EGTA (EGTA) or 0.45 mM $CaCl_2$ and 500 µM L-NMMA (L-NMMA) for 10 min at 37°C. eNOS activity was estimated as pmol/min of L-[^{3}H] citrulline formed in the reaction, normalised to protein content. B: Ca^{2+}-dependency of eNOS activity in intact cells. Cell monolayers, grown in the presence or absence of doxycycline, were incubated for 15 min at 37° C in a medium containing L-[^{3}H] arginine without other additions (control), with 100 µM ATP (ATP) or with 100 µM ATP and 500 µM L-NAME (ATP + L-NAME). eNOS activity was estimated as in A. C: Cytochemical analysis of NADPH tetrazolium blue reductase activity of eNOS in cells grown in the presence (a) or absence (b) of doxycycline in the culture medium. Preparations were examined in bright field. A dark precipitate is visible in cells induced to express eNOS (b), whereas non-induced cells are barely visible (a). Photography, digital acquisition, and printing were exactly the same for the two panels. Bar, 15 µm. The results shown are from one experiment representative of four consistent ones. D: cGMP generation induced by activation of eNOS. 2 x 10^6 Aδ cells, grown in the presence or absence of doxycycline, were suspended together with 0.5 x 10^6 PC12 cells and incubated for 15 min at 37°C under the conditions described in B. cGMP accumulation was estimated by a radioimmunoassay and normalised to protein content. Statistical probability in panels A, B and D is indicated by the asterisks and calculated vs. EGTA-containing lysates (A) or untreated control cells (B and D), whereas the crosses refer to the statistical probability in samples treated in the presence vs. absence of either L-NMMA or L-NAME (n = 4) (see Experimental Procedures for details).

Fig. 4. Effects of eNOS expression on TNF-α-induced apoptosis. Cell monolayers, grown in the presence (dox+) or absence (dox-) of doxycycline were incubated without (control) or with TNF-α (100 ng/ml) and CHX (1 µg/ml) for further 12 h. L-NAME (500 µM) was added during the incubation where indicated. Apoptosis was analysed measuring, by flow

cytometry, phosphatidyl serine exposure and DNA staining with propdium iodide. The left-hand panel shows the exposure of phosphatidyl serine, assessed using fluorescein-iso-thiocyanate labelled-annexin V (x axis, arbitrary units). The increase in annexin V-positive cells after treatment with TNF-α/CHX is lower in eNOS-expressing cells (d) than in non-induced cells (b) or eNOS-expressing cells treated with L-NAME (f). No significant annexin V staining is present in control cells not exposed to the cytokine and the protein synthesis inhibitor (a, c and e). The right-hand panel shows the DNA content analysed by flow cytometry measuring the binding of propidium iodide (x axis, arbitrary units). In these experiments HeLa cells were not synchronised; accordingly, G0/G1, S and G2/M phases were present as already described for these cells (55). The sub-G1, hypodiploid DNA peak, characteristic of apoptosis, is clearly detectable in cells treated with TNF-α/CHX (h, l and n) with respect to untreated controls (g, i and m) and is lower in eNOS-expressing cells (l). Incubation with L-NAME resulted in a sub-G1 peak similar to the one observed in non-induced cells (n). The results shown are from one out of four representative experiments. M1 indicates the region considered for the statistical analyses of Table II.

Fig. 5. Effect of TNF-α on eNOS activity and cGMP generation. A: dependency of NOS activity on TNF-α and drugs interfering with sphingolipid metabolism. Cell monolayers, grown in the presence (dox+) or absence (dox-) of doxycycline, were incubated for 3 h at 37°C in culture medium with 10 μM Fum (4th bar), 50 μM PDMP (5th bar), or without other additions (first 3 bars). Cells were then treated for a further 15 min at 37°C in a medium containing L-[^{3}H] arginine with or without either TNF-α (100 ng/ml), L-NAME (500 μM), Fum or PDMP as indicated. NOS activity was estimated as described in Fig. 3 B. B: effects of TNF-α and drugs interfering with sphingolipid metabolism on cGMP generation. 2 x 10^{6} Aδ cells, grown in the presence or absence of doxycycline, and incubated with Fum or PDMP as in A, were suspended together with 0.5 x 10^{6} PC12 cells and treated for 15 min at 37°C with or without either TNF-α, L-NAME, Fum and PDMP as described in panel A.

cGMP accumulation was estimated as described in Fig. 3 D. Statistical probability vs. untreated control cells is indicated by the asterisks, that of samples incubated with TNF-α in the presence vs. absence of either L-NAME, PDMP or Fum by crosses, both calculated as described under Experimental Procedures (n = 4).

Fig. 6. Schematic model for modulation of the TNF-α triggered apoptosis by NO and ceramide. Activation by TNF-α of TNF-RI results in receptor trimerisation and recruitment of TRADD and then FADD, which leads to activation of caspase-8. The ensuing ceramide generation (56,57), acts as an amplifying factor of the response to TNF-α, by increasing TRADD recruitment. Moreover, it may contribute to apoptosis by triggering other signalling events (58). Ceramide, however, stimulates also eNOS activity and the generated NO down-regulates the accumulation of the lipid messenger. In addition, NO may counterbalance the apoptogenic effect of ceramide also because of its action on additional events involved in TNF-α-induced apoptosis (see text for details). The functional coupling between eNOS and TNF-RI might be facilitated by the subcellular localisation of the enzyme and the receptor, both known to concentrate in the caveolae at the plasma membrane (34,59,60).

Table I: effects of eNOS expression on the TNF-α-induced conversion of MTT into formazan

	control	TNF-α/CHX
dox +	0.159±0.003	0.115 ± 0.001 $^{***}_{+++}$
dox + / L-NAME	0.160 ± 0.002	0.113 ± 0.003 ***
dox -	0.161 ± 0.004	0.149 ± 0.001 *
dox - / L-NAME	0.162 ± 0.005	0.118 ± 0.002 $^{***}_{+++}$

HeLa Aδ cells, seeded in 6-well plates (10 x 10^4 cells/cm^2), were cultured in the presence (dox +) or absence (dox-) of doxycycline and then treated with TNF-α (100 ng/ml) and CHX (1 μM) for 6 h or left untreated (control). When indicated, this treatment was carried out in the presence of L-NAME (500 μM). Cell were then washed and incubated with MTT (2.4 mM) for a further 3 h. Conversion of MTT into its derivative formazan by mitochondrial dehydrogenases was measured as described under Experimental Procedures. Statistical probability vs. controls is indicated by the asterisks, calculated as described under Experimental Procedures (n = 4). The differences between values observed after TNF-α/CHX treatment in dox + vs. dox- and dox- / L-NAME vs. dox- (indicated by the crosses) are highly significant ($P < 0.001$ in both cases).

Table II: effects of eNOS expression on the TNF-α-induced exposure of phosphatidyl serine and formation of hypodiploid DNA

	annexin V staining		propidium iodide staining	
	control	TNF-α/CHX	control	TNF-α/CHX
dox +	5.1 ± 0.3	41.3 ± 1.6 *** +++	16.8 ± 0.9	66.2 ± 3.4 *** ++
dox+ / L-NAME	4.98 ± 0.6	45.3 ± 2.5 ***	18.5 ± 1.3	65.3 ± 4.9 **
dox -	5.5 ± 1.1	21.2 ± 1.3 ***	16.2 ± 0.8	46.2 ± 2.3 ***
dox- / L-NAME	6.6 ± 1.2	42.8 ± 2.0 *** +++	16.9 ± 0.9	60.3 ± 3.5 *** ++

HeLa Aδ cells, cultured in the presence (dox+) or absence (dox-) of doxycycline were treated with TNF-α (100 ng/ml) and CHX (1 μM) for 12 h, or left untreated (control), before analysis of annexin V and propidium iodide staining by flow cytometry as described under Experimental Procedures. Values represent the percentage of cells measured in the M1 regions, defined as shown in Fig. 4. Statistical probability vs. controls is indicated by the asterisks, that of dox+ vs. dox- and dox-/L-NAME vs. dox- cells after TNF-α/CHX treatment by the crosses, both calculated as described under Experimental Procedures (n = 4).

Table III: effects of TNF-α, PDMP and fumonisin B1 on ceramide accumulation in HeLa dox+ cells.

	control	TNF-α
dox+	13.5 ± 0.1	33.3 ± 2.0 ***
dox+ / PDMP	15.5 ± 1.4	57.8 ± 3.1 *** ++
dox+ / Fum	12.4 ± 1.2	18.8 ± 0.2 ** ++

HeLa Aδ cells, cultured in the presence of doxycycline were incubated for 3 h with or without PDMP (50 μM) or Fum (10 μM) prior to a 15 min treatment in the absence (control) or presence of TNF-α (100 ng/ml). Ceramide was measured as described under Experimental Procedures. Values are expressed as pmol/mg proteins. Statistical probability vs. controls is indicated by the asterisks, that of cells incubated with PDMP or Fum vs. non-incubated cells after TNF-α/CHX treatment by the crosses, both calculated as described under Experimental Procedures (n = 3).

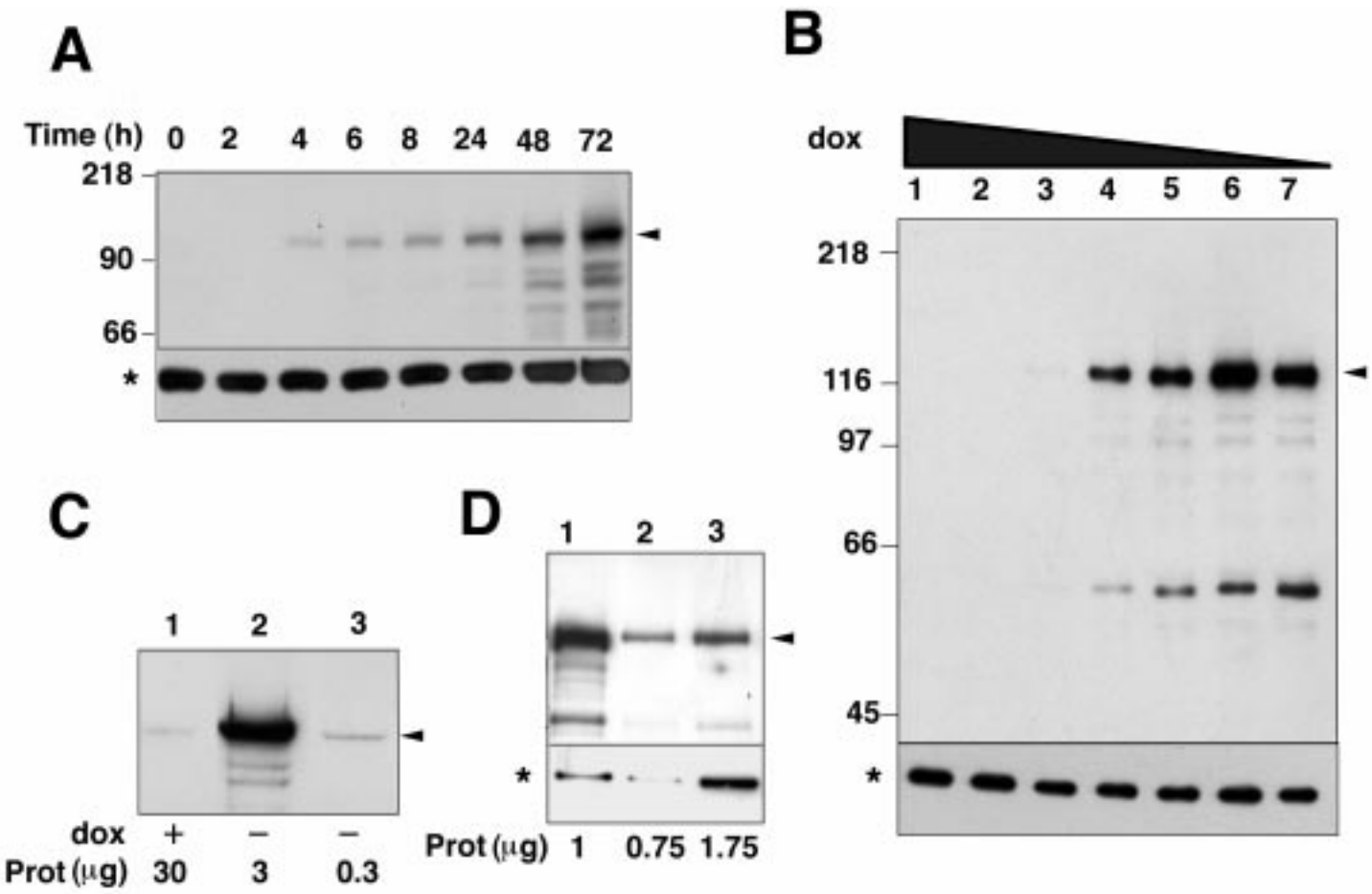

Figure 1

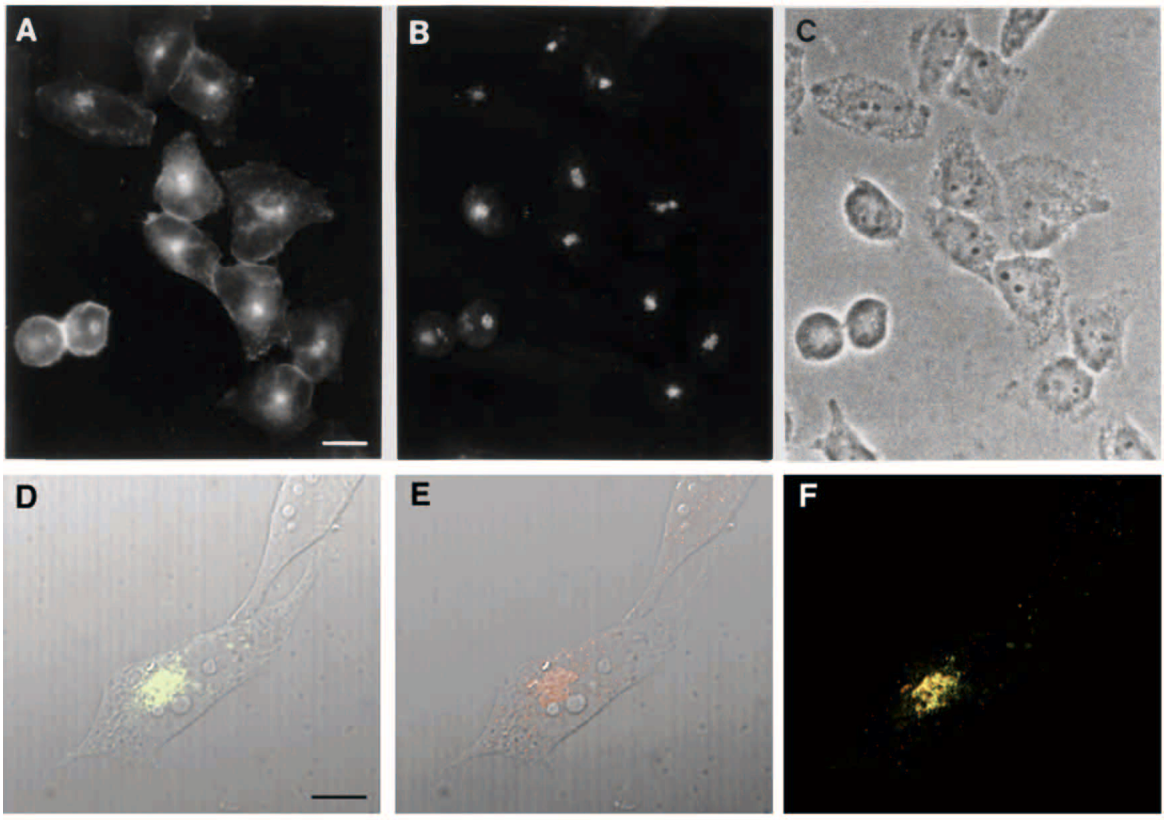

Figure2

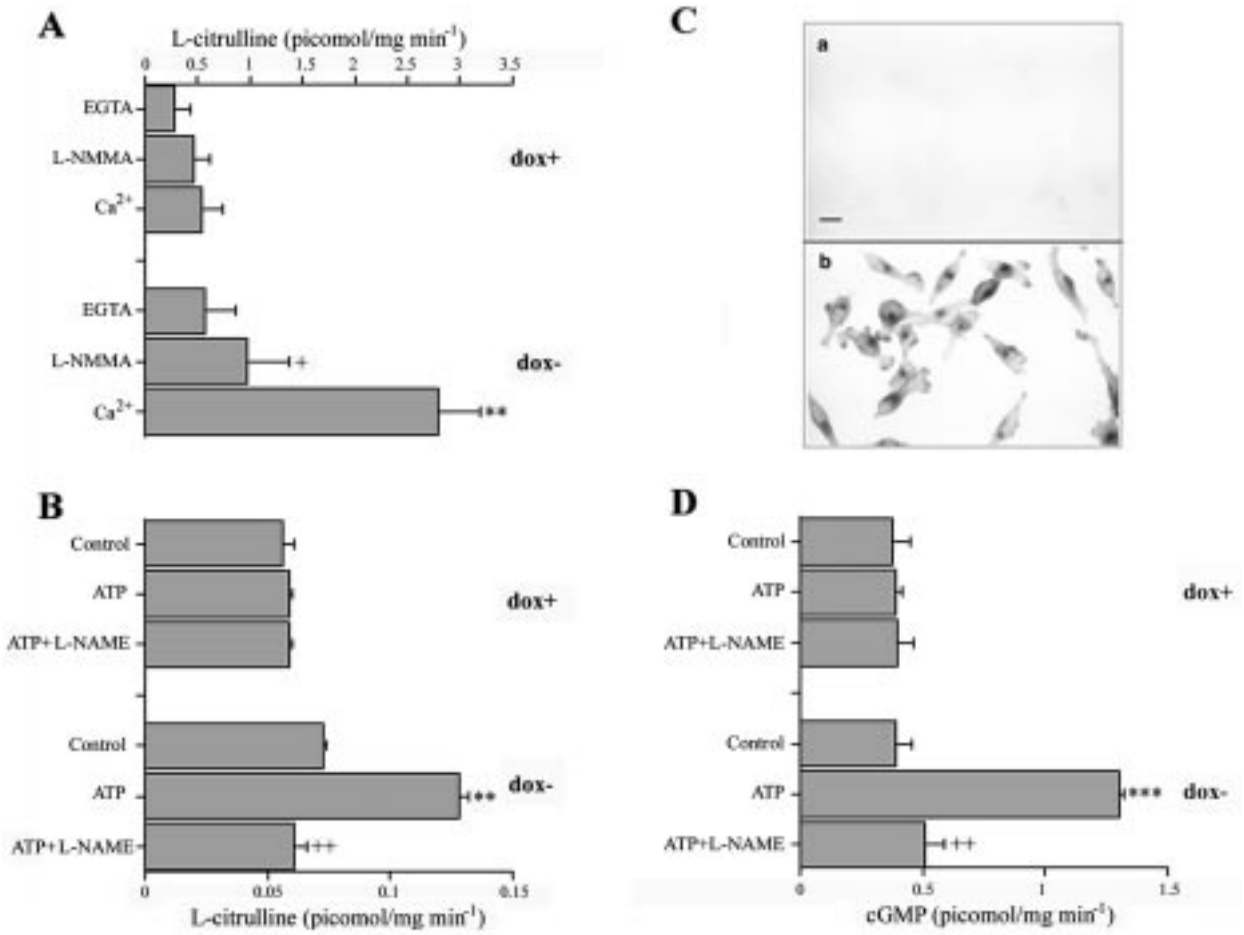

Figure 3

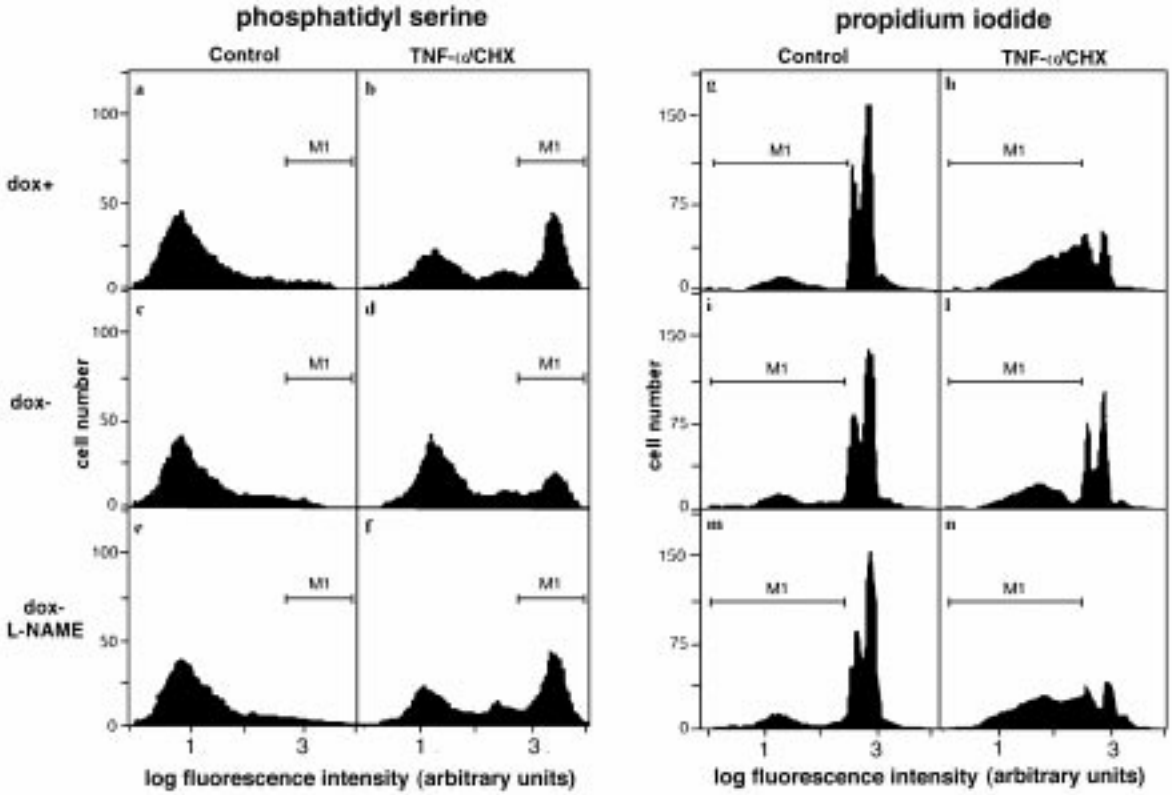

Figure 4

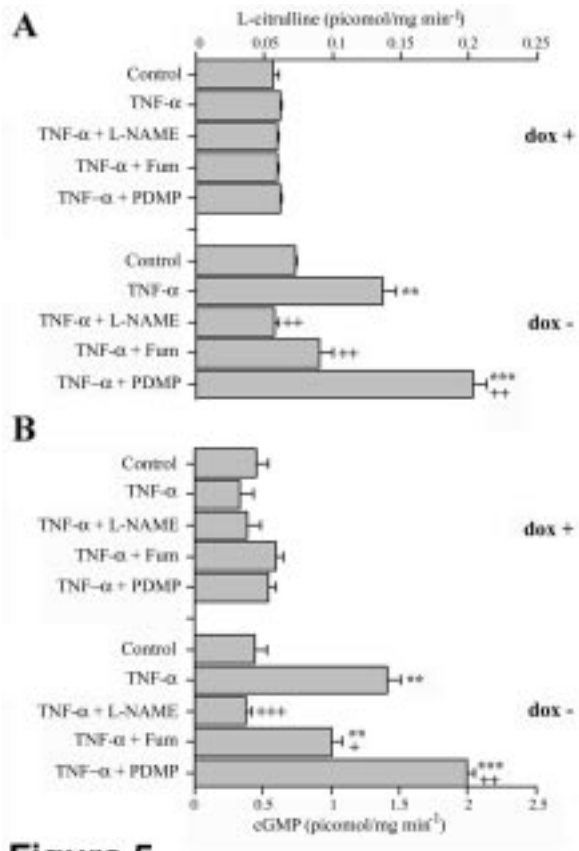

Figure 5

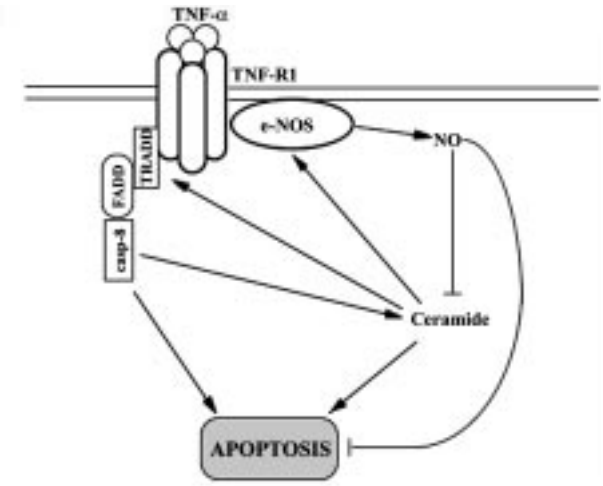

Figure 6

Activation of the endothelial nitric oxide synthase by tumour necrosis factor-alpha: A novel feed-back mechanism regulating cell death

Stefania Bulotta, Rico Barsacchi, Domenicantonio Rotiroti, Nica Borgese and Emilio Clementi

J. Biol. Chem. published online November 20, 2000
